Flexible *Ab Initio* Boundary Conditions: Simulating Isolated Dislocations in bcc Mo and Ta

C. Woodward* and S. I. Rao*

Materials and Manufacturing Directorate, Air Force Research Laboratory, Wright Patterson Air Force Base, Dayton, Ohio 45433-7817

(Received 4 January 2001; published 13 May 2002)

We report the first *ab initio* density-functional study of the strain field and Peierls stress of isolated $\langle 111 \rangle$ screw dislocations in bcc Mo and Ta. The local dislocation strain field is self-consistently coupled to the long-range elastic field using a flexible boundary condition method. This reduces the mesoscopic atomistic calculation to one involving only degrees of freedom near the dislocation core. The predicted equilibrium core for Mo is significantly different from previous atomistic results and the Peierls stress shows significant non-Schmid behavior as expected for the bcc metals.

DOI: 10.1103/PhysRevLett.88.216402 PACS numbers: 71.15.–m, 61.72.Lk, 62.20.Fe

Plastic deformation in metals is mediated by the motion of line defects (dislocations) that produce a long-range stress field. Many material properties (e.g., strength and ductility) are directly related to the structure and mobility of dislocations. Continuum elasticity has been very successful in describing these long-range fields. However, close to the dislocation center (core) there are large lattice distortions and the elastic solution diverges [1]. Atomistic simulations demonstrate that local forces at the dislocation core and their coupling to the applied stress can have a dramatic effect on structural properties. Currently there are few methods which can probe the electronic structure which produces the forces at the dislocation core. Because of this there is a poor understanding of the "chemistry of deformation."

In this Letter we report the first *ab initio* technique, the first-principles Greens function boundary condition (FP-GFBC) method, for self-consistently coupling the strain field produced by a line defect to the long-range elastic field of the host lattice. The problem is divided into two parts: a robust solution for the nonlinear dislocation-core region and a solution for the long-range elastic response. Solving these individual problems is straightforward and by iteratively coupling the two solutions we can efficiently solve for the strain field in all space. A plane-wave pseudopotential method has been adapted to use this technique and we have applied it to study $a/2\langle 111 \rangle$ screw dislocations in the bcc transition metals. The objective is to demonstrate an efficient electronic structure method for predicting how the critical stress, required to move a dislocation (Peierls stress), changes for different elemental metals having the same crystal structure.

Physical and computational issues.—Modeling extended defects in metals requires a self-consistent coupling of the defect center to the long-range elastic field. Edge or screw dislocations produce a stress field which is proportional to the inverse of the distance to the dislocation core [1]. In conventional atomistic methods a surface is used to accommodate the discontinuity in the lattice produced by the Burgers vector (b), and a large buffer region ($\sim 10^4$ atoms) is used to isolate the dislocation core from the surrounding static lattice. Simulation cells of this size are beyond the scope of current electronic structure methods.

Alternatively, dislocation dipoles can be used to localize the cut in the lattice produced by the dislocation. Several groups have used reciprocal space methods to simulate arrays of dislocation dipoles in order to minimize the effects of the long-range stress field [2–4]. Unfortunately the dislocation dipole array imposes an artificial symmetry which is not necessarily consistent with the symmetry of the dislocation core. Also, the bcc transition metals are expected to have extended dislocation cores which are quite sensitive to the image stresses produced by the boundary conditions [5,6].

We describe an alternative *ab initio* method which is designed to self-consistently couple the core region to the long-range stress field. The FP-GFBC method is an adaptation of the lattice GFBC method which has been used in atomistic calculations of two- and three-dimensional dislocation structures in simple metals and ordered intermetallics [6,7]. In this method the dislocation core is embedded in a lattice Greens Function region that produces a stress field consistent with the response function of the bulk metal. These calculations show that dislocations can be contained in very small simulation cells without compromising the fidelity of the final core configuration. In the first-principles implementation the lattice and elastic Greens function are derived from reference electronic structure calculations. The response functions are used to optimize the ionic positions based on the Hellmann-Feynman forces. The current application is an example of a two-dimensional GFBC method; generalizing the method for three-dimensional defect centers is straightforward.

Ab-initio method.—Calculations were performed using the *ab initio* total energy and molecular-dynamics program VASP (Vienna *ab initio* Simulation Package) developed at the Institut für Theoretische Physik of the Technische Universität Wien [8–11]. Ultrasoft Vanderbilt pseudopotentials [9,12] were used to approximate the electron-ion interactions. We expand the wave functions in a plane-wave basis, and bands near the Fermi surface are partially occupied using finite temperature broadening

($k_BT = 0.1$ eV). Calculations for Mo and Ta used energy cutoffs of 233.1 and 218.5 eV with 4 and 8 special k points, respectively. With these choices the total energies are converged to within 0.01 eV/atom. Predicted lattice and elastic constants (Table I) are consistent with previous norm-conserving pseudopotential calculations and are within expected error when compared to experimental measurements [13,14]. Small shear strains in the $\langle 111 \rangle$ direction produce a shear stress proportional to G [$G = (C_{11} - C_{12} + C_{44})/3$]. The value of G found for Ta is significantly more accurate than that found for C_{44} and errors in G of 15% are acceptable for this study.

Deriving the lattice Greens function.—To determine the lattice Greens function we construct the elastic Greens function based on the elastic constants for a given pseudopotential and crystal structure (Table I) [6]. The resulting elastic Greens function is used to define the displacement field near an atom undergoing a test force along each lattice direction ($F_i = 0.1$ eV/Å). We construct a supercell using the lattice vectors of the target simulation (e.g., the dislocation coordinate system) and the predicted displacement field. The atomic positions are then optimized using the VASP code which has been modified to include the corresponding test force. The Hellmann-Feynman forces are converged to less than 0.01 eV/Å. We find that the final displacement field converges to the elastic Greens function solution approximately 5 Å from the atom undergoing a test force.

Evaluation of possible simulation cells.—We have explored several techniques for terminating an isolated dislocation within the supercell. In both approaches the volume containing material is divided into three distinct regions. In the first approach a disk of material, with a thickness of one periodic length along $\langle 111 \rangle$ ($a\sqrt{3}/2$), is used to enclose the dislocation core. A vacuum region is then used to isolate the dislocation from its periodic images in the (111) plane (Fig. 1a). The second approach uses the same dislocation-cell geometry; however, the vacuum region is eliminated by extending region 3 to the boundaries of the supercell (Fig. 1b). The supercell walls normal to the $\langle 11\bar{2} \rangle$ and $\langle \bar{1}10 \rangle$ directions form domain boundaries (DB). Supercell size and geometry are chosen to minimize the overlap of atomic charge densities in the DB while maintaining the correct lattice parameters and atomic density. The charge dipoles produced in this region produce far smaller perturbations in the charge density than a free surface. By using DB the initial forces in the core region converge to the accuracy of the electronic structure method in two-thirds of the volume needed for calculations using a vacuum region. Since the electronic structure method scales with cell volume the computational effort is significantly reduced by using simulation cells with domain boundaries. Finally, the two methods converge to the same result with increasing cell size. The limitations of employing a vacuum region will also be apparent in real-space electronic structure calculations of line defects.

Applying the flexible boundary condition method.—In the current implementation of the FP-GFBC method the dislocation is centered within two concentric cylindrical regions using the geometry illustrated in Fig. 1b. Region 3 is used to isolate the dislocation core from the DB region. The method proceeds as follows: (i) Initial atomic positions are approximated by the anisotropic elastic solution for the dislocation line [15]. (ii) The atomic positions within region 1 are optimized using the Hellmann-Feynman forces generated from the electronic structure method. This produces incompatibility forces for atoms in region 2. (iii) These forces are relieved by displacing all the atoms in the simulation cell according to the Greens function solution:

$$u_i^m = \sum_{j,n} G_{ij}^{mn}(R_{mn}) f_j^n , \qquad (1)$$

where the indices m, n denote atoms, the indices i, j denote the Cartesian components, $R_{mn} = R_n - R_m$ and f_j^n are the Hellmann-Feynman forces. (iv) Steps (ii) and (iii) are repeated until the desired convergence is achieved. Step (iv) is required because region 1 contains a line defect and the Greens functions used in step (iii) are based on the response of the perfect lattice. Also, optimization of the atomic positions in steps (ii) and (iii) are applied in reciprocal and real space, respectively. This effectively isolates the dislocation from the strain field of its periodic images. Finally, we note that at each step the atoms are displaced according to the Hellmann-Feynman forces produced by the electronic structure method.

TABLE I. Calculated and measured lattice parameters, bulk modulus, and elastic molduli (Mbar) for bcc Mo and Ta [13]. Results under column labeled NC-PP are from earlier norm-conserving pseudopotential calculations [14].

	Mo			Ta		
Property	VASP	NC-PP	Expt.	VASP	NC-PP	Expt.
a (Å)	3.100	3.121	3.147	3.230	3.246	3.295
B	2.87	2.83	2.70	2.14	2.20	1.93
C_{11}	5.04	4.70	4.79	2.91	3.04	2.66
C_{12}	1.79	1.87	1.65	1.75	1.82	1.58
C_{44}	0.920	1.01	1.08	0.53	0.66	0.88
G	1.39	1.28	1.41	0.56	0.62	0.65

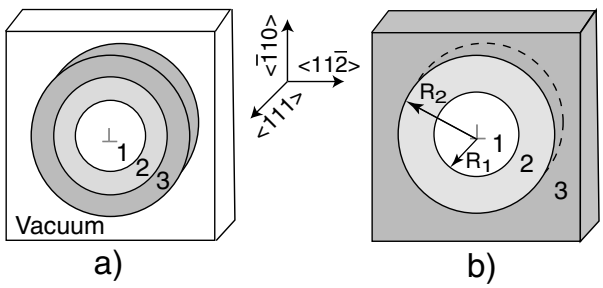

FIG. 1. Schematics of possible geometries for the simulation cells: (a) using a vacuum region and (b) using domain boundaries parallel to the dislocation line.

The convergence of the forces using this procedure is plotted in Fig. 2 for a cell of 270 Mo atoms containing a screw dislocation. The average Hellmann-Feynman force on atoms within each region is shown for the initial and final positions of the atoms in step (ii) described above. After the initial step all the forces are reduced at each step in the iterative procedure until we reach the limits in accuracy of the electronic structure method.

Core structure and convergence of cell size.—The predicted dislocation-core structure for Mo is shown in a (111) projection using differential displacement (DD) maps (Fig. 3a) [16]. We find that the predicted DD for Ta is nearly identical to that found for Mo. The arrow centered between any two atoms is the relative $\langle 111 \rangle$ displacement due to the presence of the dislocation. The arrow lengths are scaled such that a displacement of $b/3$ produces a vector that connects nearest-neighbor atoms in this projection. Figure 3b shows the equilibrium core for Mo found by using advanced many-body atomistic potentials based on modified generalized pseudopotential theory (MGPT) [17,18]. The plot is representative of previous atomistic studies which show the Mo core spreading asymmetrically about a central point on the three conjugate (110) planes [5,17] producing an approximate threefold rotational symmetry ($C3$). This is in contrast to the current results, where the dislocation core spreads evenly about a central point producing full $D3$ symmetry. In order to rule out the $C3$ geometry as a possible global-energy minimum we relaxed the equilibrium atomistic core using the *ab initio* method. In all cases the dislocation core relaxed to a core with full $D3$ symmetry [19]. First-principles simulations of an infinite array of dislocation quadrapoles produce a similar equilibrium core structure for Mo [4].

Earlier atomistic studies have shown that variations in core symmetry can be characterized quantitatively by calculating the polarization [20]. The polarization is derived from the atomic displacements in the core region and converges rapidly with increasing cell size. In Mo we find the polarization converged to within 8% of the asymptotic value for cells with $R_2 \sim 12.1$ Å (Fig. 1b). This will be discussed in more detail in a later paper.

Lattice friction stress.—The stress required to move a screw dislocation is determined by applying pure shear or uniaxial stress on simulation cells with $R_2 \sim 12.1$ Å (168 atoms). Plastic deformation in the bcc metals is quite complex; slip can occur in any of the $\langle 111 \rangle$ directions on a variety of slip planes. Also, these materials violate Schmid's law which states that glide on a given slip system will occur when the resolved shear stress on that system reaches a critical value (the Peierls stress).

Figure 4 shows the Peierls stress (i.e., the critical resolved shear stress) predicted for Mo and Ta as a function of the angle (χ) between the plane with the maximum shear stress and the (110) plane. Similar results from (MGPT) atomistic simulations are shown for comparison [17,18]. We find good agreement between the methods for pure shear stress on the (112) plane in the twinning sense ($\chi = -30$). However, we find significant differences in Ta for stress on the (110) plane ($\chi = 0$) and in both metals for pure shear on the (112) plane in the antitwinning sense ($\chi = 30$). Experimental measurements of the Peierls stress for pure shear are quite difficult. However, in 1969, using a novel mounting jig, Guiu measured critical stresses (τ) for a pure shear stress in Mo at 77 K and found $\tau(\chi = 30)/\tau(\chi = -30) > 1.5$ [21]. Here the *ab initio* results give a ratio of 1.8.

We find that in Mo the dislocation glides primarily on the (110) plane with the maximum shear stress, while in Ta the dislocation moves on alternating (110) planes to produce an effective (211) slip plane. These results are generally consistent with previous atomistic simulations [5,17,18]. However, contrary to previous results, we find that the projected symmetry of the equilibrium dislocation core (i.e., $D3$ or $C3$) is not strongly correlated with the preferred primary slip plane. Schmid's law implies that the Peierls stress varies as $1/\cos\chi$ for a (110) primary slip plane, this dependence is illustrated in Fig. 4a as a solid line. Both the current predictions and the MGPT results show significant non-Schmid effects for pure shear. Also, we predict a large tension-compression asymmetry (Fig. 4a) for uniaxial stress applied along (010) and (011) in bcc Mo. This non-Schmid behavior is observed experimentally

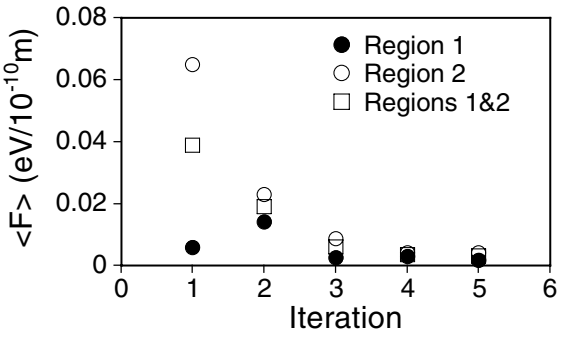

FIG. 2. Convergence of the atomic forces using the FP-GFBC method.

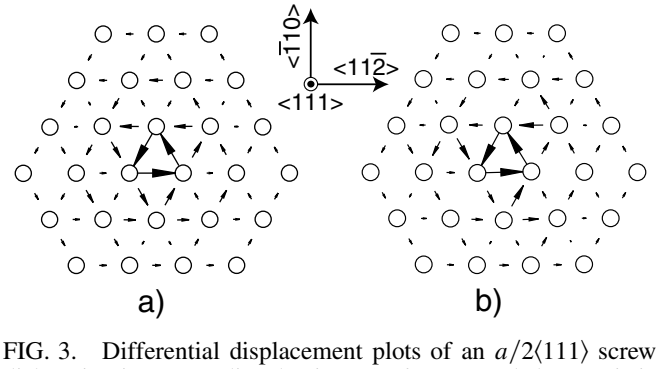

FIG. 3. Differential displacement plots of an $a/2\langle 111 \rangle$ screw dislocation in Mo predicted using (a) *ab initio* and (b) atomistic methods [17].

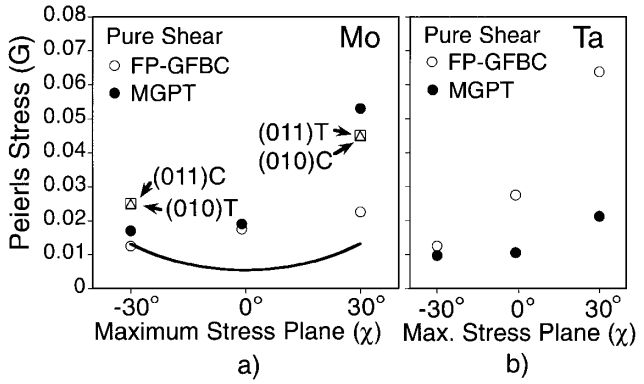

FIG. 4. Predicted Peierls stress in (a) Mo and (b) Ta as a function of the angle (χ) between the maximum resolved shear stress plane and the (110) plane. The Peierls stress is in units of the shear modulus in the $\langle 111 \rangle$ direction (G).

and is attributed to the effects of nonglide stress on the dislocation core [5].

As noted in other studies the predicted Peierls stress is a factor of 2 or 3 times greater than that observed in low temperature experiments [4,17,18]. However, the critical stress has been estimated using a highly idealized model of slip, an infinite, straight dislocation moving over the Peierls barrier. This predicted critical resolved shear stress should be considered as an upper bound to the Peierls stress. In general we expect that the material will yield at lower stresses, even at low temperatures where kink dynamics are reduced. The low temperature experimental measurements may reflect the activation of new sources or the unpinning of the small but finite population of mixed and edge segments.

We find that the MGPT simulations underestimate the Peierls stress in Ta and overestimate the Peierls stress in Mo. This contradicts the recent assertions made by Ismail-Beigi and Arias regarding the scale of the Peierls stress produced by these atomistic potentials [4]. Our *ab initio* results show that the Peierls barrier is large (compared to the fcc metals), consistent with conventional models of crystal plasticity in the bcc metals. These initial results suggest that properly constructed many-body atomistic potentials can capture some qualitative features of plastic deformation in the bcc transition metals [5,17,18]. However, predicting differences between elemental metals (e.g., Ta and Mo) will require improved interaction models or *ab initio* methods such as the one described here.

A flexible boundary condition method has been used to isolate a single dislocation in an *ab initio* supercell calculation. The method employs a lattice Greens function that was derived using a simple well-defined procedure and a widely available *ab initio* method. The atomic positions within the supercell containing the dislocation were optimized using an iterative scheme based on the Hellmann-Feynman forces. The method converges rapidly with increasing cell size and is relatively straightforward to implement. The method was used to estimate the Peierls stress for pure shear and uniaxial stress in two bcc transition metals. Almost forty years ago Hirsch proposed that nonplanar and extended dislocation cores were responsible for the unusual plastic deformation observed in the bcc transition metals [22]. This study is the first *ab initio* confirmation of the origin of the non-Schmid behavior in these materials.

We thank J. Moriarty, D. M. Dimiduk, L. H. Yang, M. Asta, M. Baskes, and V. Vitek for many useful discussions over the course of this project. This work was supported by the DOE under Contract No. B346019, the AFOSR under Contract No. F33615-96-C-5258, and by a grant of computer time from the DOD High Performance Computing Modernization Program, at the ASC-MSRC, on the IBM-SP3. The work was performed at the U.S. Air Force Research Laboratory, Materials and Manufacturing Directorate, Wright-Patterson AFB.

*Present address: UES Inc., 4401 Dayton-Xenia Rd., Dayton, Ohio 45432.

[1] J. P. Hirth and J. Lothe, *Theory of Dislocations* (McGraw-Hill, New York, 1982).
[2] J. R. K. Bigger *et al.,* Phys. Rev. Lett. **69**, 2224 (1992).
[3] X. Blase, K. Lin, A. Canning, S. G. Louie, and D. C. Chrzan, Phys. Rev. Lett. **84**, 5780 (2000).
[4] S. Ismail-Beigi and T. A. Arias, Phys. Rev. Lett. **84**, 1499 (2000).
[5] M. S. Duesbery and V. Vitek, Acta Mater. **46**, 1481 (1998).
[6] S. I. Rao, C. Hernandez, J. P. Simmons, T. A. Parthasarathy, and C. Woodward, Philos. Mag. A **77**, 231 (1998).
[7] S. I. Rao, T. A. Parthasarathy, and C. Woodward, Philos. Mag. A **79**, 1167 (1999).
[8] G. Kresse and J. Hafner, Phys. Rev. B **47**, 558 (1993).
[9] G. Kresse and J. Hafner, Phys. Rev. B **49**, 14 251 (1994).
[10] G. Kresse and J. Furthmueller, Comput. Mater. Sci. **6**, 5 (1996).
[11] G. Kresse and J. Furthmueller, Phys. Rev. B **55**, 11 169 (1996).
[12] D. Vanderbilt, Phys. Rev. B **41**, 7892 (1990).
[13] G. Simmons and H. Wang, *Single Crystal Elastic Constants* (MIT Press, Cambridge, MA, 1971); W. B. Pearson, *Handbook of Lattice Spacing and Structures of Metals* (Pergamon, New York, 1967).
[14] C. Woodward *et al.,* Phys. Rev. B **57**, 13 459 (1998); P. Soderlind *et al.,* Phys. Rev. B **61**, 2579 (2000).
[15] A. N. Stroh, Philos. Mag. **3**, 625 (1958).
[16] V. Vitek, R. C. Perrin, and D. K. Bowen, Philos. Mag. **21**, 1049 (1970).
[17] S. I. Rao and C. Woodward, Philos. Mag. A **81**, 1317 (2001).
[18] L. H. Yang, Per Soderlind, and J. A. Moriarty, Philos. Mag. A **81**, 1355 (2001).
[19] C. Woodward and S. I. Rao, Philos. Mag. A **81**, 1305 (2001).
[20] M. S. Duesbery *et al.,* Proc. R. Soc. London A **332**, 85 (1973).
[21] F. Guiu, Scr. Metall. **3**, 449 (1969).
[22] T. E. Mitchell, R. A. Foxall, and P. B. Hirsch, Philos. Mag. **8**, 1895 (1963).